U.S. FOOD & DRUG ADMINISTRATION
CENTER FOR DEVICES AND RADIOLOGICAL HEALTH

Synthetic sources of image data and their utility

Anant Agrawal, PhD
Daniel X. Hammer, PhD

Division of Biomedical Physics, Office of Science and Engineering Laboratories,
Center for Devices and Radiological Health, US Food and Drug Administration

Office of Science and Engineering Laboratories

183 FEDERAL EMPLOYEES
Up to 180 visiting scientists

140 Projects
In 27 laboratories and Program Areas

400/year
Peer reviewed presentations, articles, and other public disclosures

2,500/year
Premarket Regulatory consults

75
Standards and conformity assessment committees

70%
Staff with post graduate degree

55,000 ft²
Lab facilities

2

DC AO/OCT Community

NIH NEI
- PIs: Tam, Cukras, Chew, Wong, Wiley, et al.
- Capabilities: multi-λ. AOSLO+ICG, FDML-based multimodal AO-OCT (Fall 2019)
- Clinical focus: AMD, inherited retinal diseases, hydroxychloroquine toxicity, RPE stem cell therapies, clinical endpoints

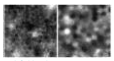

Dark-field and ICG AOSLO images of human RPE cells (Tam et al.)

Minimum intensity SDOCT analysis of hydroxychloroquine toxicity (Cukras et al.)

FDA
- PIs: Hammer, Liu, Agrawal
- Capabilities: mAO, FDML-based AO-OCT (Fall 2019)
- Focus: Glaucoma, AO biomarkers, AO phantoms

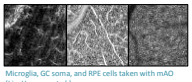

Microglia, GC soma, and RPE cells taken with mAO (Liu, Hammer et al.)

UMD
- PI: Saeedi
- Clinical focus: Glaucoma, blood flow

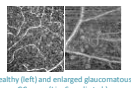

Healthy (left) and enlarged glaucomatous GC soma (Liu, Saeedi et al.)

...growing AO and OCT capabilities and impact for clinical translation and regulatory science

Motivation

How best to validate and standardize AO and OCT performance?

- ISO OCT standard is limited
- No clinical gold standards to compare to
  - OCT is three-dimensional and not directly relatable to standard fundus imaging
  - OCT angiography employs fundamentally different technological characteristics than dye angiography
  - Unprecedented and exceptional capabilities in AO and OCT
    - Other functional biomarkers (e.g., phase-based)
    - AO provides uniquely high spatial resolution, coupled with dynamic and personalized imaging

4

Synthetic data sources

Phantoms ⇨ Physical tools for imaging performance evaluation

Model eyes ⇨

Synthetic images ⇨ Software tools associated with machine learning

5

Phantom: basic concept

Precision test target
Imaging performance principles

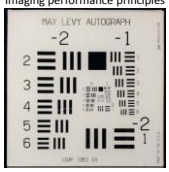

+

Known physical properties of tissue
(geometry, dimensions, scattering/absorption)

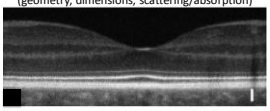

=

PHANTOM: Physical model with controlled properties for tissue-relevant performance characterization

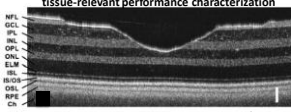

Baxi et al, JBO 2014

Quantify image quality metrics
Compare devices
Track performance
Calibrate measurements
Access underlying physics

⇨ **Streamline device development, evaluation, regulation**

6

Commercially available OCT phantoms

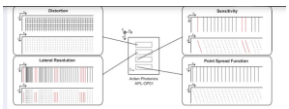

Multi-parameter phantom
For measuring several important imaging performance metrics
www.ardenphotonics.com

Retina-like phantom
www.rowetechnical.com

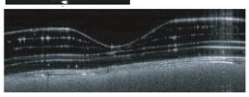

Phantoms for retinal OCT imaging

3D point spread function phantom
Agrawal et al, BOE 2012

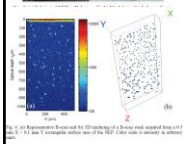

Baxi et al, JBO 2014

Improved macula phantoms
Lee et al, JBO 2015
Bowden lab, formerly Stanford Univ.

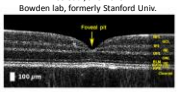

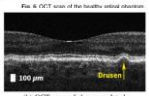

(b) OCT scan of dry age-related macular degeneration

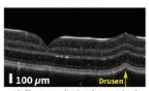

(d) Phantom replicating dry age-related macular degeneration

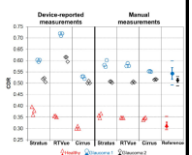

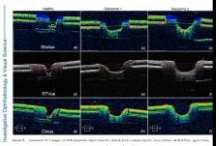

Optic nerve head phantoms
Agrawal et al, IOVS 2016

Multimodal AO photoreceptor phantom

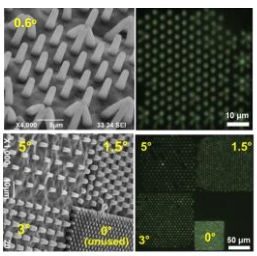

3D-printed cylinders encapsulated in silicone

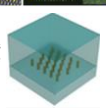

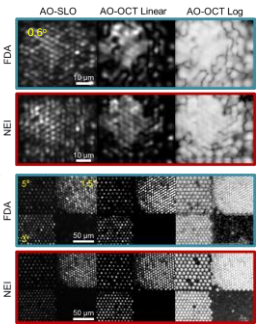

Kedia et al, Optics Letters 2019

Model eyes

OEMI-7
www.ocularinc.com

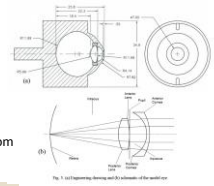

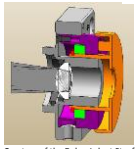

High-precision calibrated model eye

Courtesy of the Dubra Lab at Stanford University and Moondog Optics

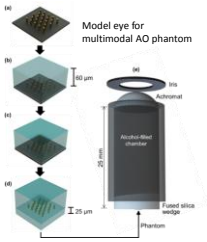

Model eye for multimodal AO phantom

Kedia et al, Optics Letters 2019

Model eye – OCT standard

ISO 16971:2015(E) Ophthalmic instruments — Optical coherence tomograph for the posterior segment of the human eye

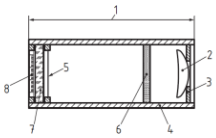

Key

1 length approx. 17 mm
2 lens, f = 17 mm
3 aperture, diameter 6 mm
4 tube
5 single filament with 100 µm diameter (has to be tight)
6 neutral density filter
7 glass plane, 1 mm thick
8 scale with reference marks for field size

Software-based synthetic image formation and usage

Data augmentation

Model-based data generation

Data augmentation for manual segmentation

Retinal optical coherence tomography image enhancement via deep learning

KERRY J. HALUPKA,[1,*] BHAVNA J. ANTONY,[1] MATTHEW H. LEE,[1] KATIE A. LUCY,[2] RAVNEET S. RAI,[2] HIROSHI ISHIKAWA,[2] GADI WOLLSTEIN,[2] JOEL S. SCHUMAN,[2] AND RAHIL GARNAVI[1]

[1]IBM Research, Level 22/60 City Rd, Southbank, Victoria, Australia
[2]Department of Ophthalmology, NYU Langone Eye Center, New York University School of Medicine, New York, NY, USA

Healthy	PSNR	SSIM	MS-SSIM	MSE
Raw	26.82±0.67	0.62±0.04	0.79±0.02	136.67±22.43
BM3D	31.17±1.27	0.74±0.04	0.88±0.02	51.53±17.29
DD-CDWT	31.21±1.19	0.75±0.04	0.89±0.02	51.22±15.92
CNN-WGAN	31.83±1.21	0.77±0.03	0.92±0.01	44.52±14.34
CNN-MSE	**32.28±1.27**	**0.78±0.03**	**0.92±0.01**	**40.28±13.44**
Glaucoma	**PSNR**	**SSIM**	**MS-SSIM**	**MSE**
Raw	25.46±0.67	0.58±0.04	0.76±0.02	188.32±52.53
BM3D	29.12±1.12	0.74±0.03	0.88± 0.03	83.34±44.76
DD-CDWT	29.44±1.18	0.74±0.03	0.89±0.03	77.84±46.15
CNN-WGAN	29.92±1.27	0.76±0.03	0.91±0.02	72.85±46.07
CNN-MSE	**30.21±1.12**	**0.78±0.03**	**0.92±0.03**	**70.04±44.91**

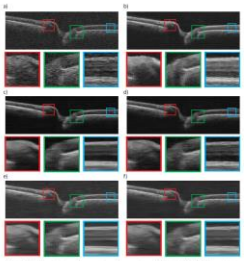

Fig. 3. OCT Image from a glaucomatous volume captured by Cirrus HD-OCT Scanner (a), and corresponding 6-frame averaged image (b). The result of post-processing of (a) with CNN-MSE (c), CNN-WGAN (d), BM3D (e), and DD-CDWT (f). Three zoomed in, colour coded sections are shown below each B-scan (best viewed in colour).

13

Data augmentation for algorithm training

Choroid segmentation from Optical Coherence Tomography with graph-edge weights learned from deep convolutional neural networks

Xiaodan Sui[a,b,c], Yuanjie Zheng[a,b,c,*], Benzheng Wei[d], Hongsheng Bi[b,c], Jianfeng Wu[e], Xuemei Pan[e], Yilong Yin[f], Shaoting Zhang[g]

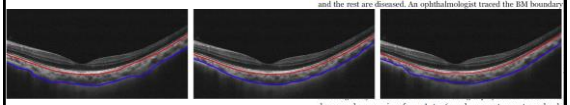

3.1. Data set and data augmentation

Macular-centered 3D EDI-OCT volumes (1536 × 496 × 49 voxels with a resolution of 5.8 × 3.9 × 123.9 μm³) were obtained using the Heidelberg Spectralis instrument (Heidelberg Engineering, Heidelberg, Germany) from both oculus sinister and oculus dextrus of 42 normal subjects and 31 patients diagnosed with macular edema, aged between 34 and 68 years old. The research protocol was approved by the local Institutional Review Aboard, and written informed consent was obtained from all participants. From these OCT volumes, we manually chose 912 B-scans which are in good quality and bear a full view of the choroid, retina and sclera. Among these B-scans, 618 scans are normal and the rest are diseased. An ophthalmologist traced the RM boundary

degree values varying from 1 to 6 and parameters set randomly between [0 1] (with a similar way to our previous work [43]). They were all finally scaled to a value within [0.51.5]. Adding the combination of these geometric and photometric variations result in an augmented training set with a size of 23,972 images. All images were resized to 768×256 by using a bilinear interpolation before feeding into our CNN architecture. Here, the scale factors applied to rows and columns are a little different in order for a convenient usage in our CNN model.

14

Model-based data generation

Statistical Models of Signal and Noise and Fundamental Limits of Segmentation Accuracy in Retinal Optical Coherence Tomography

Theodore B. DuBose, David Cunefare, Elijah Cole, Peyman Milanfar, *Fellow, IEEE*, Joseph A. Izatt, and Sina Farsiu, *Senior Member, IEEE*

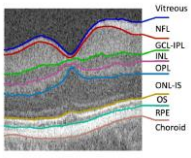

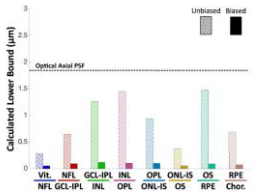

15

Summary

- A number of non-clinical physical tools (phantoms and model eyes) have been developed for AO and OCT imaging, mostly in prototype form
- Community consensus needed to identify most important data to obtain with physical tools
  - Imaging performance figures of merit
  - Measurement accuracy
  - System calibration during longitudinal studies
  - Post-processing traceability
- Software-based synthetic image usage in AO and OCT is quite nascent; data augmentation has potential to enhance training of AI/deep learning algorithms

16